

# Generation and orientation of organoxenon molecule H-Xe-CCH in the gas phase

Viktoriya Poterya, Ondřej Votava, and Michal Fárník\*

*J. Heyrovský Institute of Physical Chemistry,  
Academy of Sciences of the Czech Republic, Prague 8, Czech Republic*

Milan Ončák and Petr Slavíček†

*Department of Physical Chemistry, Institute of Chemical Technology,  
Technická 5, Prague 6, Czech Republic*

Udo Buck

*Max-Planck Institut für Dynamik und Selbstorganization,  
Bunsenstr. 10, D-37073 Göttingen, Germany*

Břetislav Friedrich

*Fritz-Haber-Institut der Max-Planck Gesellschaft,  
Faradayweg 4-6, D-14195 Berlin, Germany*

(Dated: December 19, 2007)

## Abstract

We report on the first observation of the organoxenon HXeCCH molecule in the gas phase. This molecule has been prepared in a molecular beam experiment by 193 nm photolysis of an acetylene molecule on Xe<sub>n</sub> clusters ( $\bar{n} \approx 390$ ). Subsequently the molecule has been oriented via the pseudo-first-order Stark effect in a strong electric field of the polarized laser light combined with the weak electrostatic field in the extraction region of a time-of-flight spectrometer. The experimental evidence for the oriented molecule has been provided by measurements of its photodissociation. For comparison, photolysis of C<sub>2</sub>H<sub>2</sub> on Ar<sub>n</sub> clusters ( $\bar{n} \approx 280$ ) has been measured. Here the analogous rare gas molecule HArCCH could not be generated. The interpretation of our experimental findings has been supported by *ab initio* calculations. In addition, the experiment together with the calculations reveals information on the photochemistry of the HXeCCH molecule. The 193 nm radiation excites the molecule predominantly into the 2<sup>1</sup>Σ<sup>+</sup> state, which cannot dissociate the Xe-H bond directly, but the system evolves along the Xe-C coordinate to a conical intersection of a slightly non-linear configuration with the dissociative 1<sup>1</sup>Π state, which then dissociates the Xe-H bond.

## I. INTRODUCTION

The noble gas elements were long thought to be exempt from any chemical bond formation until 1962, when the first compound containing Xe atom was synthesized.<sup>1</sup> In the past decades, noble gas chemistry has made a great progress. Among the most interesting noble gas compounds belong their hydrides of the type H-Rg-Y, where Rg is the rare gas atom (Ar, Kr or Xe) and Y is an electronegative atom or group. These species have been first observed experimentally in 1995.<sup>2,3</sup> Surprisingly, compounds of this type paved the way towards the first and so far the only neutral argon compound HArF.<sup>4</sup> The bonding in these molecules has partly an ionic character with the positive charge localized on the H-Rg group and the molecular residue Y being negative,  $(\text{H-Rg})^+\text{Y}^-$ . However, the role of the covalent bonding in these molecules is also essential. Until today, about twenty HRgY hydrides have been identified. The fast development of the field is summarized in recent reviews.<sup>5-7</sup> The HRgY species can also contain an organic moiety as predicted theoretically by Lundell et al.<sup>8</sup> The first experimental evidence for organoxenon hydride formed from acetylene (HXeCCH) was reported in 2003.<sup>9,10</sup>

Typically these molecules are prepared by UV photolysis or radiolysis of various HY molecules in Rg matrices and subsequently identified by IR spectroscopy of a characteristic vibrational band, the strong H-Rg stretching mode. In the matrix, the generation of the molecule usually proceeds in two steps: first the atomic H and the rest fragments of Y are produced by the HY molecule dissociation, and then the temperature is raised to activate the migration of the H-atom in the matrix and the molecules are formed in the recombination reaction  $\text{H}+\text{Rg}+\text{Y}\rightarrow\text{HRgY}$ . However, an alternative *direct formation mechanism* has been observed in some cases, e.g., after the photolysis of HCl in a Kr matrix.<sup>11,12</sup> In this case the H fragment was backscattered from an Rg atom in the next Rg-layer, recoiled to a transition state of the H-Rg-Y geometry, and recombined to the HRgY molecule. Such processes have been simulated by molecular dynamics with the non-adiabatic transitions included.<sup>13</sup> The time scale for such fast processes is of the order of a few picoseconds. The HRgY molecule generated in the direct process can be immediately photolyzed with the next photon arriving with the UV radiation used to photolyze the HY molecule. Therefore, the total yield of the HRgY molecules generated in the matrix by the direct process is smaller than for the molecules generated after the matrix annealing.

Rare gas hydrides in the gas phase have been first observed in the group of U. Buck.<sup>14–16</sup> The molecules are prepared by photodissociation of HY molecules on free Rg clusters in molecular beams. Obviously, only molecules generated by the direct mechanism can be produced in this case. The experimental evidence for the rare gas molecule in this experiment is its orientation by a pseudo-first-order Stark effect<sup>17</sup> and subsequent photolysis of the oriented molecule. The measured time-of-flight spectra of the H-fragments from the randomly oriented HY molecules are isotropic, while the fragments from the oriented HRgY molecules contribute to the spectra anisotropy, as will be briefly discussed below. More details on the generation and orientation of HRgY molecules in cluster beam experiments can be found in our recent review.<sup>18</sup> A fairly high degree of orientation is required to identify the molecule, which depends on molecular parameters such as the anisotropy of dipole polarizabilities. Since there is a trade off between these parameters, the stability of the molecule and their photochemical properties, so far only two of these species (HXeI and HXeCl) could be identified in the gas phase. We note that in our method a single laser pulse can be utilized for (i) dissociation of the HY molecule and preparation of HRgY, (ii) orienting the HRgY molecule, (iii) photodissociation of this molecule, and (iv) ionization of the outgoing hydrogen fragment.

Here we report on the first observation of the free organoxenon hydride HXeCCH generated by the photolysis of an acetylene molecule  $C_2H_2$  on a  $Xe_n$  cluster. Previously the molecule has been observed after photolysis<sup>9</sup> and, alternatively, fast electron bombardment<sup>10</sup> of acetylene in solid Xe matrices. This molecule has also been prepared in argon and krypton matrices<sup>19</sup> and its complex with  $CO_2$  has recently been characterized.<sup>20</sup> In relevance to the present study also the photodissociation of HXeCCH molecule at 193 nm irradiation has been reported in Ref. 20. In all these experiments the molecule was generated in solid state matrices, with the indirect process mentioned above after annealing of the irradiated sample. Interestingly, it has been predicted that molecular crystals of HXeCCH should be a stable phase.<sup>21</sup>

The output of the present experiment is a kinetic energy release spectrum originating from oriented species. We have used the support of theoretical calculations to confirm that the signal originates from the HXeCCH molecule. Theoretical calculations also bring further insight into the processes of formation and decomposition of the molecule. In particular we need to find whether (i) HRgY can be formed under the experimental conditions, (ii) HRgY

is stable on the timescale of the experiment, (iii) HRgY can be oriented, (iv) HRgY can be photoexcited, and (v) what are the reaction channels of HRgY after photoexcitation and what is the energetics of the excitation processes. We have therefore explored the potential energy surface of the HYRg/HRgY system at several levels of theory. The ground state has been explored with density functional theory (DFT), Møller-Plesset perturbation theory of second order (MP2), multi-state complete active space perturbation theory (MS-CASPT2) and multi-reference configuration interaction (MRCI) levels, the excited states have been mapped using equation of motion - coupled cluster (EOM-CCSD), MS-CASPT2 and MRCI levels of theory. It has been shown in several studies<sup>22-24</sup> that calculations covering a significant portion of the correlation energy, including the static correlation, is vital for reliable estimates of HRgY compounds. This is especially true for the H+Rg+Y dissociation channel. We have also used theoretical calculations to obtain the molecular parameters on the basis of which we can discuss the degree of orientation of the molecule in our experiment.

The HXeCCH molecule has been reported to be stable by 1.46 eV with respect to the separation to the fragments H+Xe+C<sub>2</sub>H.<sup>5</sup> Although the decomposition to Xe+HCCH is exoergic by 4.5 eV, it is prohibited by a 2.18 eV high and extremely broad barrier along the H-Xe-C bending coordinate. Two other species have been isolated in the matrices:<sup>9,10</sup> HXeCC and HXeH. Furthermore, HCCXeCCH molecule has been predicted theoretically.<sup>25</sup> We discuss the possible occurrence of these species in our experiment. We have also investigated the photolysis of acetylene on Ar<sub>n</sub> clusters. We show that in this case the rare gas molecule HArCCH is not generated or stabilized.

## II. EXPERIMENT

### A. Experimental apparatus

The experiment was performed in an apparatus for photodissociation studies of molecules in cluster environments<sup>26</sup> used previously at the Max-Planck Institute in Göttingen, and installed recently at the J. Heyrovský Institute of Physical Chemistry in Prague. More details of the experiment relevant to the generation of oriented molecules can be found in the review Ref. 18 and references therein.

Briefly, the  $Rg_n$  cluster beam was produced by a supersonic expansion of neat Rg gas through a nozzle of conical shape (60  $\mu\text{m}$  diameter,  $30^\circ$  opening angle, 2 mm length). The mean cluster sizes were determined by the expansion pressure and nozzle temperature according to Hagenau's empirical law<sup>27,28</sup> and are summarized in Tab. I. After passing through a skimmer followed by a differentially pumped vacuum chamber, the cluster beam entered a pick-up cell filled with the acetylene gas, where the  $C_2H_2$  molecules were attached to the clusters.

The molecules on clusters were photolyzed in a detection chamber equipped with a two-stage time-of-flight spectrometer of the Wiley-McLaren type (WMTOF). Subsequently, the H-fragments were ionized, and the spectrometer was used to record their time-of-flight distributions (TOF). For this purpose the WMTOF was operated in the so called low-field mode with a small electrostatic field applied to extract the ions toward the detector. With the extraction, ions could be detected with initially zero velocity or even a velocity vector pointing away from the detector and their velocities could be analyzed. The extraction field intensity was essential for the HRgY molecule orientation as discussed below, and is given in Tab. I.

The acetylene molecules were photolyzed by the 193 nm radiation from an ArF/ $F_2$ -Excimer laser (Lambda: Compex 102). The laser pulses were repeated at a frequency of 10 Hz with a pulse duration of 20 ns. The emitted light was polarized using a thin film polarizer (TFP), and sent into the detector chamber perpendicularly to both, the cluster beam and the WMTOF axis. To orient the HXeCCH molecule the light was polarized parallel ( $0^\circ$ ) with respect to the WMTOF axis. The effective laser intensity was approximately  $3.3 \times 10^{10} \text{ Wcm}^{-2}$  in the interaction region.

After the dissociation the H fragment ionization proceeded with 243.07 nm laser beam via the one-color, resonance enhanced multiphoton ionization (REMPI) in a 2+1 excitation scheme. This wavelength was generated by mixing the fundamental of a Nd:YAG laser (Quanta Ray GCR-5) with the frequency doubled output of a dye laser (LAS, LDL 20505) operated at 630.3 nm, and pumped by the second harmonic of the Nd:YAG laser. The laser pulses were repeated at a frequency of 10 Hz with a pulse duration of 5 ns. The polarization of the ionization laser light was again parallel to the WMTOF axis ( $0^\circ$  polarization). The effective laser intensity in the focal spot was approximately  $3.1 \times 10^{10} \text{ Wcm}^{-2}$ , quite similar to the intensity of the 193 nm radiation (Tab. I).

Essential to these experiments was the beam overlap. The time synchronization of the two laser beams was achieved by triggering the excimer laser by the Nd:YAG laser pulses via a pulse delay generator. The spatial overlap of the two focussed laser beams with the intersection point of the cluster beam and the WMTOF axis was achieved by measuring the signal from a test system  $(\text{HBr})_n/\text{Ar}$  system. Since the indication for the photolysis of oriented molecules was asymmetry of the TOF spectra, great attention was paid to careful laser beam alignment to obtain the symmetric shape of the TOF spectrum of the test system. The tight laser light focusing into a small spot in the interaction region was important, since the molecule alignment and orientation depend strongly on the electric field intensity of the laser light, as outlined below.

The measured TOF spectra were converted to the kinetic energy distribution (KED) of the H atom after the photodissociation. The transformation was carried out by a complete Monte-Carlo (MC) simulation of the particle trajectories considering the parameters of the photodissociation process, the molecular beam data, the finite interaction volume, the geometry of the experiment and the electronic response of the detector.<sup>29,30</sup>

## B. Formation and orientation of H-Rg-Y molecules

The detailed mechanism of the HRgY molecule generation in the cluster beam experiment and its orientation has recently been described elsewhere.<sup>18</sup> Therefore only a brief recapitulation is given here. Following the HY molecule dissociation in the  $\text{Rg}_n$  cluster the generated H fragment atom can recoil from the neighboring Rg atoms and recombine with the Y group, with one additional Rg atom inserted, to create the HRgY molecule. During this process the excess energy deposited into the  $\text{Rg}_n$  cluster evaporates its constituents which results in a bare HRgY molecule or, alternatively, a molecule with a few Rg atoms attached.<sup>16,18</sup>

After the HRgY molecule is created, it is oriented in the combined weak electrostatic field  $\epsilon_S$  used to extract the fragment ions and the strong electric field of the plane-polarized laser  $\epsilon_l$ . In the present experiment both these fields were aligned parallel to the WMTOF axis to observe the molecule orientation. First, the principal axis of the strongly polarizable HXeY molecule is forced to align in the direction of the  $\epsilon_l$  vector by the interaction of the

polarizability anisotropy with the laser field, given by

$$V = -(2\pi I_l/c)(\alpha_{\parallel} - \alpha_{\perp})\cos^2\theta + \alpha_{\perp}. \quad (1)$$

Here  $I_l$  is the laser intensity  $I_l = (c/4\pi)\epsilon_l^2$ ,  $\alpha_{\parallel}$  and  $\alpha_{\perp}$  are the polarizabilities parallel and perpendicular to the molecular axis, and  $\theta$  is the angle between the molecular axis and the field polarization, which is parallel to the WMTOF axis in the present geometry. The molecule alignment can be characterized in terms of a dimensionless parameter<sup>17</sup>

$$\Delta\omega = 10^{-11}\Delta\alpha(\text{\AA}^3)I_l(W\text{cm}^{-2})/B(\text{cm}^{-1}), \quad (2)$$

where  $\Delta\alpha = \alpha_{\parallel} - \alpha_{\perp}$  and  $B$  is the rotational constant of the HRgY molecule. When aligned, the molecule can still point in two opposite directions in the polarization plane.

The additional weak extraction electric field  $\epsilon_S$  of the WMTOF turns this alignment into orientation. Interaction of this field with the permanent dipole moment of the linear molecule  $\mu$  is given by

$$V = -\mu\epsilon_S\cos\theta_S, \quad (3)$$

where  $\theta_S$  is the polar angle between the molecular axis and the direction of the electrostatic field. This interaction can be again characterized by a dimensionless parameter

$$\omega = 0.0168\mu(\text{Debye})\epsilon_S(kV\text{cm}^{-1})/B(\text{cm}^{-1}). \quad (4)$$

For sufficiently large values of  $\omega$  the rotor  $J$ ,  $M$  states of the molecule can be confined to oscillate about the field direction in the so-called pendular states comprised of linear combinations of states with the same  $M$  and different  $J$ . In a combined parallel static electric field and a non-resonant laser field even a weak static field can induce a strong orientation by the pseudo-first-order Stark effect.<sup>17,31,32</sup> The orientation of the molecular axis in a given state is characterized by its orientation cosine  $\langle\cos\theta_s\rangle$ : the greater the orientation cosine the smaller the angular amplitude of the molecular axis librations in the field. The orientation cosine as a function of  $\Delta\omega$  and  $\omega$  has been calculated elsewhere (e.g. see Fig. 6 in Ref. 17). For the lowest tunneling doublet the  $\tilde{J} = 0, M = 0$  and  $\tilde{J} = 1, M = 0$  states are oriented opposite with respect to one another.  $\tilde{J}$  is the angular momentum quantum number of the field-free rotor state that adiabatically correlates with the field-oriented hybrid. Therefore their mixture would exhibit alignment only. Orientation can be achieved if a single state is selected. The strong cooling of the nascent HRgY molecule necessary to obtain the pure



lowest  $\tilde{J} = 0, M = 0$  state of a tunneling doublet is provided by the cluster environment which leads to a very small zero point motion of the created HRgY molecule.<sup>15</sup> The molecular parameters necessary for the calculation of the orientation cosine for the present molecule have been calculated as outlined below and are summarized in Tab. II.

After the HRgY molecule is formed and oriented it can be photodissociated. Successively the fragment H atoms are ionized by the 2+1 REMPI process and detected with the WMTOF spectrometer. Since at the  $0^\circ$  laser beam polarization the HRgY is oriented with the H atom pointing towards the detector, the resulting arrival times of the nascent protons are shorter than the corresponding times of the zero kinetic energy fragments. Consequently, the measured time-of-flight (TOF) spectrum is asymmetric with respect to the zero kinetic energy fragment peak with more intensity on the shorter arrival time side. Thus the spectrum asymmetry is an indication for the photodissociation of an oriented molecule in our experiment.

### III. CALCULATIONS

In order to justify our interpretation of the asymmetry of the TOF spectra from photodissociation of  $C_2H_2/Rg_n$  system in terms of the oriented HXeCCH (or HXeCC or HArCCH) molecule, we have mapped out the potential energy surface of both the ground and several excited states of the HXeCCH and HXeCC systems. We have explored the stability of the generated hydride molecules as well as the dynamical events following the HXeCCH photoexcitation. Furthermore, we have calculated the molecular data needed to evaluate the orientation angle of the molecule, i.e. the principal components of the polarizability tensor  $\alpha_{\parallel}$  and  $\alpha_{\perp}$ , the permanent dipole moment  $\mu$ , and the rotational constant  $B$ . These calculations were performed for both possible xenon molecules HXeCCH and HXeCC, as well as for the HArCCH species, since the  $C_2H_2/Ar_n$  system has been measured for a comparison.

The anisotropy of the polarizability, rotational constants and dipole moments were calculated at the MP2 and DFT levels, with aug-cc-pVTZ basis set<sup>33</sup> on the light atoms (H, C, Ar). For xenon, we have used corresponding aug-cc-pVTZ-PP basis based on small-core relativistic pseudopotential.<sup>34</sup> In the pseudopotential used (ECP28MDF), 28 electrons have been treated explicitly. The MP2 method with a basis of a triple zeta quality provides a reasonable compromise between computational costs and accuracy. The average atom po-

larizabilities calculated at this level for the H, C and Xe atoms have deviated at most 4 % with respect to the experimental data.<sup>35</sup> The polarizability anisotropy of the xenon dimer ( $\text{Xe}_2$ ) has been calculated as  $1.24 \text{ \AA}^3$ , in complete agreement with experimental value of  $1.3 \pm 0.3 \text{ \AA}^3$ .<sup>36</sup> DFT/B3LYP calculations with the same basis lead to somewhat worse agreement with the experiment for the atomic polarizabilities, however, still generally with an error less than 10%. We can expect MP2 and DFT methods to be working well for the closed shell systems  $\text{C}_2\text{H}_2$ ,  $\text{HXeCCH}$  and  $\text{HArCCH}$ . We have treated the open shell  $\text{HXeCC}$  radical using the unrestricted formalism of the MP2 and DFT methods. In this case we should be concerned about the spin contamination. This problem is usually less pronounced at the DFT level.<sup>37</sup> This is shown to be also the case here. The spin eigenvalue at the MP2 calculation has been calculated to be as large as 1.10 compared to 0.75 for a pure doublet state. With the DFT/B3LYP approach, the  $S^2$  was 0.77. We have therefore calculated  $\text{HXeCC}$  molecular properties at the DFT level.

The ground potential energy surface of the  $\text{HXeCCH}$  molecule has been explored at the DFT, MP2, MS-CASPT2 and MRCI levels of theory. Aug-cc-pVDZ (or Aug-cc-pVDZ-PP for Xe) basis and the same effective core potential as described above have been utilized. Optimization of the stationary points (minima and transition states) has been done with DFT, MP2 and MS-CASPT2 methods, MRCI energies have been then calculated for MS-CASPT2 optimum geometries. It has been shown that the MP2 method systematically overestimates the stability of the rare gas hydrides.<sup>23</sup> This is due to bond breaking during the isomerization or decomposition processes. The transition state of the reaction  $\text{HCCXeH} \rightarrow \text{HCCH} \cdot \cdot \text{Xe}$  has been found at DFT, MP2 and MS-CASPT2 levels and confirmed by the IRC calculation.

Potential energy surfaces in the excited states have been described at MS-CASPT2 and MRCI levels. EOM-CCSD excitation energies in the Franck-Condon geometries have been calculated for comparison. The aug-cc-pVDZ basis has been used for all calculations in the excited states. The  $\text{C}_{2v}$  symmetry has been exploited for potential energy scans in linear geometries with 2/0/2/2 electrons in 4/0/1/1 orbitals for  $\text{A}_1/\text{A}_2/\text{B}_1/\text{B}_2$  irreducible representations (*irreps*), no orbitals were frozen. For interpolation calculations, the  $\text{C}_s$  symmetry has been employed with 4/2 electrons in 5/2 orbitals for  $\text{A}'/\text{A}''$  *irreps*. For cases where the symmetry has not been applied, the active space with six electrons in six orbitals (6/6) has been used for the multi-reference calculations. Five states have been averaged

in the MS-CASPT2 and MRCI calculations of the HXeCCH system: Ground state of  $^1\Sigma^+$  symmetry, two excited  $^1\Pi$  states and two excited  $^1\Sigma^+$  states. For the HCCH $\cdots$ Xe complex, two  $^1\Sigma^+$  and two  $^1\Sigma^-$  states have been averaged. For the interpolation between the two local minima, 6 and 3 states in A' and A'' *irreps* of the  $C_s$  symmetry group were averaged. The described active space selection and state averaging lead to inclusion of all important orbitals and electronic states and was found to be consistent with results for larger 10/10 active space and also with the EOM-CCSD values. The excitation energies for both HXeCCH and HCCH $\cdots$ Xe molecules are robust with respect to the active space choice and symmetry constraints. The first three excitation energies of the HCCH $\cdots$ Xe molecule do not differ from the experimental values of acetylene excitation energies by more than 0.1 eV at the MRCI level.<sup>38</sup> The same active space has also been used for the HArCCH molecule. For calculation of the HXeCC radical, the 5/6 active space has been used. Davidson correction has been added to the MRCI energies to account for the lack of size extensiveness.

The electronic spectrum of the HXeCCH molecule has been calculated at the MRCI level with no symmetry applied in 6/6 active space. The spectrum has been estimated by a Monte Carlo procedure utilizing reflection principle,<sup>39</sup> with 400 *ab initio* points randomly selected from the vibrational harmonic ground state Wigner distribution.

Molecular constants have been calculated using the Gaussian03 programme suite,<sup>40</sup> all the other calculations have been performed with the Molpro06 code.<sup>41</sup>

#### IV. EXPERIMENTAL RESULTS

Fig. 1 shows the two TOF spectra of H-fragments from the photolysis of acetylene on Ar $_n$ ,  $\bar{n} = 280$ , clusters (a), and on Xe $_n$ ,  $\bar{n} = 390$ , clusters (b). Both spectra are similar with the maximum at about 3.98  $\mu$ s, which corresponds to the arrival time of the zero kinetic energy H-fragments. In the C $_2$ H $_2$ ·Ar $_n$  spectrum (a) there are two almost symmetric peaks on both sides of the main maximum. It should be noted, that a slight asymmetry of the TOF spectrum arises even if a completely isotropic orientation of the dissociating molecule is assumed. The slight asymmetry results from the larger detector acceptance angle for the H-fragments ejected in the direction of the detector compared to the acceptance angle for the H-fragments ejected in the opposite direction, which have to be turned around by the extraction field to fly towards the detector. This very small asymmetry can be accounted for

by the MC simulation of the dissociation process in the WMTOF considering the explicit geometry as outlined in the experimental section. The fit of the experimental data using this simulation procedure for the  $C_2H_2$  molecule is shown by the solid line in the Fig. 1 (a).

In contrast, the bottom spectrum (b) could not be successfully fitted assuming the symmetric dissociation in all directions towards and away from the detector. The TOF spectrum asymmetry here is more pronounced and, in addition, the shoulder at the shorter arrival times is not only higher than the shoulder on the other side but also wider, extended to shorter times. A reasonable fit could be only achieved assuming the spectrum to be composed of two contributions: (i) a symmetric part assuming the symmetric dissociation in directions towards and away from the detector, the thinner full line (note that the resulting TOF spectrum is still slightly asymmetric even for this "symmetric" component, as in the Ar case above); and (ii) an asymmetric part resulting in the dashed line and the shaded area below. The later spectrum can only arise from a dissociation of a molecule preferentially oriented in the direction towards the detector. There are only two candidates for such molecules which can be generated from  $C_2H_2$  on  $Xe_n$ :  $HXeCCH$  and  $HXeCC$ , as will be discussed below.

From the TOF spectra fits in Fig. 1 the H-fragment KEDs are obtained shown in Figs. 2 and 3. The circles in Fig. 2 correspond to the KED of H-fragments used to fit the TOF spectrum in Fig. 1 (a) from the photolysis of acetylene on  $Ar_n$ . The triangles correspond to the fit of the "symmetric" part of the TOF spectrum in Fig. 1 (b), i.e. the KED from the  $C_2H_2$  photolysis on  $Xe_n$ . Both spectra were normalized to the same area and the upper spectrum was arbitrarily shifted for clarity. The asymmetric TOF part in Fig. 1 (b) has been fitted with the KED shown in Fig. 3, which is due to the photolysis of the oriented molecule. This KED has been normalized together with the KED of the "symmetric" part in Fig. 2 to keep their ratio as obtained from the fit (note the different y-axis scale in Fig. 2 and 3).

## V. DISCUSSION

The KEDs in Fig. 2 correspond to the dissociation of  $C_2H_2$  molecules on the rare gas clusters  $Ar_n$  and  $Xe_n$ . First, it is worth noting that these distributions extend to significantly higher energies than the kinetic energies of H-fragments from photodissociation of bare

$\text{C}_2\text{H}_2$  molecules at 193 nm.<sup>42</sup> The KED of the molecular H-fragment has two close maxima at around 0.2 eV and ends at approximately 0.7 eV (see Ref. 42). Our spectra, on the other hand, peak at slightly higher energies (0.3-0.5 eV) and extend to approximately 2 eV, which means a significant amount of internal excitation of the  $\text{C}_2\text{H}_2$  molecule prior to the dissociation in the cluster. This excitation can be justified by the *cage effect* in the cluster: the  $\text{C}_2\text{H}_2$  molecule is excited by the arriving photon but the cluster prevents its dissociation. After a partial energy relaxation the  $\text{C}_2\text{H}_2$  molecule, which is still vibrationally hot, is photolyzed by the next photon, resulting in H-fragments with some excess kinetic energy corresponding to the vibrational excitation. Such a process is only facilitated by the cluster cage, and therefore cannot be observed for a bare molecule. We have further investigated this effect of caging and vibrational excitation in  $(\text{C}_2\text{H}_2)_n$  clusters of various sizes; however, it is beyond the scope of the present paper and will be discussed in more detail elsewhere.<sup>43</sup>

In the view of the above proposed scenario, it is interesting to compare the structure noticeable in the the top KED of  $\text{C}_2\text{H}_2$  on  $\text{Ar}_n$  with the vibrational energy of the symmetric C-H stretching mode in the  $\text{C}_2\text{H}_2$  molecule  $\nu_1 \approx 0.42$  eV. The arrows in Fig. 2 are spaced by this energy. Thus the extent of the KED seems to indicate an excitation with 0,1,2 and 3  $\nu_1$  vibrational quanta and even the structure of the spectrum corresponds within the experimental error to the excitation of these 4 vibrational states. This structure is less pronounced in the KED of  $\text{C}_2\text{H}_2$  on  $\text{Xe}_n$  and the spectrum seems to extend to slightly smaller energies, which can both be qualitatively interpreted, assuming a larger energy transfer from the excited molecule to the heavier Xe cage. However, it should be noted that the former KED was obtained from the TOF spectrum with a somewhat worse signal to noise ratio (see Fig. 1), as indicated also by the error bars in Fig. 2.

Finally, it should be mentioned that the effect of vibrational excitation of the molecule upon dissociation in the cluster has been observed previously for small  $(\text{HBr})_n$  clusters on the surface and inside of large  $\text{Ar}_n$  clusters.<sup>44</sup> This effect has been assigned to the vibrational excitation of the HBr molecule induced by a collision of a fast H-fragment from another photolyzed HBr molecule in the cluster. However, this mechanism cannot operate in the present case, since the kinetic energy of an H-fragment ejected from the photolyzed  $\text{C}_2\text{H}_2$  molecule ( $\sim 0.2$  eV, and 0.7 eV at most) is insufficient to excite the higher vibrational states of  $\text{C}_2\text{H}_2$ . For acetylene, the most probable mechanism would include internal relaxation following the photoexcitation without hydrogen dissociation.

The major focus of the present study has been the observation of the oriented rare gas molecule HXeCCH. The experimental evidence for the photolysis of an oriented molecule is the asymmetry of the measured TOF spectrum as outlined in the experimental part. While the asymmetry of the TOF spectrum in Fig. 1 (b) is not extremely pronounced, the spectrum could not be successfully fitted assuming a random symmetric orientation of the dissociating molecule, as already mentioned above. Therefore a dissociation of an oriented molecule had to be invoked, which accounts for a small part of the spectrum shown by the shaded area in Fig. 1 (b). Below we argue that the HXeCCH molecule can be prepared and stabilized upon the photolysis and at the same time this molecule can be oriented under the present experimental conditions.

The previous experiments showed that the HXeCCH molecules could be generated by the photolysis of the C<sub>2</sub>H<sub>2</sub> in Xe matrices.<sup>9,10</sup> The calculated stability of the HXeCCH molecule has been mentioned in the introduction. We have further explored the energetics of the HXeCCH formation and decomposition at several levels of theory. Ground state energies for the HCCH···Xe precursor, the HXeCCH molecule, the transition state connecting these two structures, and a separate H+Xe+CCH species are summarized in Table III. The ground and first excited states along an interpolation coordinate from the HXeCCH molecule to the transition state and further to the HCCH···Xe complex is shown in Fig. 4. The HXeCCH molecule is prevented from dissociation to Xe+HCCH by a barrier of 1.95 eV at the MRCI level. This is close to the previously reported value of 2.18 eV calculated at the MP2 level.<sup>8</sup> The dissociation is exoergic by 4.84 eV. The HXeCCH molecule is also stable with respect to the H+Xe+CCH fragments by 0.92 eV at MRCI level which is somewhat lower than previously reported MP2 value of 1.46 eV in Ref. 8. Our calculated MP2 dissociation energy provides us with a value of 1.08 eV, close to the MRCI value. However, this agreement is only achieved after projecting out higher spin components in the MP2 calculations. Without this correction dissociation energy of 1.57 eV is obtained. Note that in the transition state the separation between the ground and the first excited state is small, and thus the HXeCCH molecule could be formed from the excited precursor via intersection near the transition state. The potential energy scan could suggest that a direct rearrangement from the HCCH···Xe precursor to the transition state region can occur upon the photoexcitation. This is, however, not the case. Transition to the first excited state has only very limited oscillator strength and the higher states do not support this direct process. Above, we have

postulated the possibility of an internal conversion process following the photoexcitation of acetylene. It is therefore also possible that HXeCCH is formed on the ground state PES.

An analogous argon compound has not been observed in the matrix experiment, meaning that the molecule is either not formed or not stable. Our calculations with multireference methods (CASPT2 and MRCI) do not indicate any local minimum corresponding to the HArCCH arrangement. This is in accord with an empirical hypothesis presented in Ref. 23 that this compound should dissociate. Therefore we do not expect the HArCCH molecule to be formed upon the 193 nm (6.42 eV) excitation and even if the molecule was temporarily created, its lifetime would be extremely short. This is in full agreement with our measurements of the TOF spectrum upon the photodissociation of C<sub>2</sub>H<sub>2</sub> on Ar<sub>n</sub> clusters (Fig. 1 (a)). This spectrum can be fitted well within the experimental uncertainty assuming the photolysis of a randomly oriented molecule and no anisotropic component is present. It is interesting to note that a similar organo-argon compound, HArC<sub>4</sub>H, has been predicted to be stable at the MP2 level.<sup>45</sup> Our multireference calculations at the MRCI level again show that the stability of this compound is only a result of neglecting a significant part of correlation energy in MP2 calculations. This conclusion is consistent with CCSD(T) calculations of Li et al.<sup>24</sup>

It should be noted that in the matrix experiments the HXeCCH molecule has been observed after the annealing of the irradiated sample at 40 K, which activates the H-atom motion in the matrix. The nature of the xenon clusters is however somewhat different. The temperature is estimated to be higher (79 K)<sup>46</sup> and the atoms are moving more freely. Even solid clusters can have a liquid surface layer.<sup>47</sup> This is consistent with our observation that the HXeCCH molecule is generated in a direct process in the cluster environment.

After establishing the *stability* of the HXeCCH molecule, we will now discuss its *orientation*. Our calculations show that the HXeCCH molecule has a large value of polarizability anisotropy  $\Delta\alpha = 11.8 \text{ \AA}^3$  (see Tab. II). For comparison  $\Delta\alpha$  for the previously observed oriented molecule HXeI is  $17.8 \text{ \AA}^3$ , while it is an order of magnitude smaller for C<sub>2</sub>H<sub>2</sub> molecule  $\Delta\alpha = 1.7 \text{ \AA}^3$ . The large value of  $\Delta\alpha$ , together with the other molecular parameters summarized in Tab. II, results in  $\Delta\omega \approx 45$  and  $\omega \approx 4.1 \times 10^{-3}$  for the present experimental conditions.<sup>48</sup> This, in turn, means a high value of the orientation cosine  $\langle \cos\theta_s \rangle \approx 0.89$  resulting in the angular amplitude of the molecular axis libration motion in the field  $\theta_S^0 = \arccos\langle \cos\theta_s \rangle \approx 26.8^\circ$ . This is a reasonably high degree of orientation to be

observed. In our previous experiments we have seen evidence in the TOF spectra asymmetry for molecules with  $\theta_s^0 \approx 25^\circ$ , but we were unable to observe molecules which should have been generated but were expected to have a lower degree of orientation,  $\theta_s^0 \approx 54^\circ$ .<sup>18</sup> It may be noted that the hypothetical molecule HArCCH has very similar anisotropy parameters (see Tab. II), and therefore it could be oriented in our experiment, if it were generated. However, the symmetry of the corresponding TOF spectrum suggests that the molecule is not stable as proposed above, based on energetics reasons.

There are other species which have been identified in the matrix experiments. First, in the Ref. 9 xenon dihydride HXeH has been observed. This molecule cannot lead to an asymmetric TOF spectrum, since it has a linear structure with hydrogens pointing in the opposite directions. The same argument holds for another possible molecule, HCCXeCCH. Another rare gas molecule which has been observed in the matrix experiments is HXeCC.<sup>9</sup> The calculated value of polarizability anisotropy  $\Delta\alpha = 12.1 \text{ \AA}^3$  is close to the one found for HXeCCH. This, together with the other molecular constants outlined in the Tab. II, leads to the orientation cosine  $\langle \cos\theta_s \rangle \approx 0.89$ , i.e.  $\theta_s^0 \approx 27^\circ$ . The molecule could thus also be oriented. This molecule is protected from isomerization to HCC+Xe species by a barrier of 1.84 eV (at CASPT2 level). Therefore it can not be completely ruled out as a source of the anisotropy in the KED spectrum. Nevertheless, since the formation of this molecule requires the interaction with two photons, it is not expected to be the major species generated in the system. All other species which can lead to the spectra anisotropy (CCH radical, vinylidene) do not contain xenon atom and their polarizability anisotropies are low. Therefore, these molecules cannot be oriented.

Once the HXeCCH molecule has been *generated* and *oriented*, its *photodissociation* should be discussed. Fig. 3 shows the KED (asymmetric part) of the H-fragments after the photolysis of this molecule. The spectrum exhibits a broad maximum at around 1.2 eV and extends to about 2.3 eV. We have explored the photochemistry of the HXeCCH molecule by means of *ab initio* calculations. The ground state, first two excited states of  $^1\Pi$  symmetry (in  $C_{\infty v}$  notation) and two excited states of  $^1\Sigma^+$  symmetry have been considered. The excitation energies and oscillatory strengths of the HXeCCH molecule and the HCCH $\cdots$ Xe complex are presented in Table IV. The further discussion will be based on the MRCI values since the HXeCCH has partially multi-referential character even in the ground state and we also investigate dissociation processes.



The excitation energies for transitions to the  $1^1\Pi$  and  $2^1\Pi$  states of 5.21 and 6.53 eV are close to the 243 nm (5.10 eV) and 193 nm (6.42 eV) laser, respectively. However, the optical strength for these transitions is rather small. On the other hand, the transition dipole moment to the  $2^1\Sigma^+$  state at 6.37 eV is significantly higher. This transition could be reached by the 193 nm laser pulse. Fig. 5 shows calculated absorption spectrum for the HXeCCH molecule excitation to  $1^1\Pi$ ,  $2^1\Sigma^+$  and  $2^1\Pi$  electronic states. The spectrum of the  $1^1\Pi$  state is very broad and has a low intensity. The broad character of the spectrum reflects the dissociative nature of the corresponding PES with respect to both the Xe-H and the Xe-C coordinates (*vide infra*). The photon density at both experimental wavelengths are quite comparable ( $3\text{-}4 \times 10^{28} \text{s}^{-1} \text{cm}^{-2}$ ) and we can thus conclude that the excitation to the  $2^1\Sigma^+$  is the major channel for the photoabsorption.

Furthermore, the  $2^1\Sigma^+$  state is reached via a parallel transition which is favored for molecules aligned in the direction of the laser polarization compared to the perpendicular transitions to the  $1^1\Pi$  and  $2^1\Pi$  states. Note, however, that the molecules are trapped in the pendular states and thus not completely oriented all the time. We also cannot entirely rule out the occurrence of HXeCCH...Xe complexes in the system, which could be oriented with the Xe-H bond pointing in other directions, and thus other than parallel transitions could possibly occur for these species. On the other hand, the transition to the  $2^1\Sigma^+$  state is parallel, and therefore allowed (and also the absolute value of transition probability is highest). This again suggests that this is the major photoexcitation channel.

The dynamics following the excitation can be visualized with the potential energy curves presented in Fig. 6, where the changes of energy with Xe-H and Xe-C bond distances are plotted. At the  $1^1\Pi$  state, the system is dissociative with respect to both the Xe-H and Xe-C bond. However, since the acetylene moiety is much heavier than the hydrogen atom, most of the released kinetic energy will be deposited in the kinetic energy of the hydrogen atom. The excess energy in this case is 1.23 eV for the excitation with 243 nm laser and 2.55 eV for the excitation with the 193 nm laser. The  $2^1\Pi$  state can be reached by 193 nm laser and would transfer readily to the  $2^1\Sigma^+$  state through an intersection along the Xe-C coordinate, as can be seen in Fig. 6. None of the two  $1^1\Pi$  states can be, however, excited by a laser field polarized parallel to the molecule, as mentioned above. Furthermore, from the inspection of the absorption spectrum it is clear that the dominant photochemical pathway will start by an absorption to the  $2^1\Sigma^+$  state.

After the photoexcitation with the 193 nm, a small fraction of the wavepacket can be immediately transferred to the  $1^1\Pi$  state by an internal conversion process. Since the  $2^1\Sigma^+$  state is only available by the 193 nm laser (6.42 eV), the energy released in this process will be again 2.55 eV. This value is only slightly higher than the 2.3 eV at which the KED in Fig. 3 terminates. However, most of the initial wavepacket will for certain time evolve on the  $2^1\Sigma^+$  state. This state does not allow for the direct H-Xe dissociation at the given photon energies. Instead, the Xe-C bond starts to prolong to about 4.0 Å. During this process, the energy will be deposited mostly to the kinetic energy of the acetylene fragment. At the prolonged Xe-C distance there is available a low lying crossing seam connecting the  $1^1\Pi$  and  $2^1\Sigma^+$  states (corresponding geometries are not linear; the states have at this point no more the  $\Pi$  and  $\Sigma^+$  symmetry but they correlate to these states at linear geometries). The wavepacket then transfers to the  $1^1\Pi$  state, which is dissociative with respect to the Xe-H bond. The minimum energy conical intersection (which is also a minimum on the upper PES) is lying 1.32 eV above the Xe-H dissociation limit at this geometry of HXeCCH. This predicted excess energy (1.32 eV) corresponds well to the maximum of the kinetic energy distribution in Fig. 3. All the processes described above are very likely ultrafast, occurring on the femtosecond timescale. We therefore do not expect intersystem crossing to play an important role. However, this can be quite different for the process of the HXeCCH formation, since the dissociation of acetylene is not a direct process and triplet states are suspected to be involved.<sup>49,50</sup> The above scenario explains the observed KED of H-fragments from the HXeCCH molecule.

It ought to be mentioned that the HXeCCH molecule may be also complexed with additional Xe atoms. This can happen in the process of molecule generation and the cluster evaporation. The geometries and energetics of the  $\text{Xe}\cdots\text{HXeCCH}$  complex has been described previously.<sup>19</sup> Such a complex would change the orientation for the pendular state. In this case, even the  $1^1\Pi$  state could be reached. However, considering the absorption spectrum of HXeCCH, a contribution from the  $1^1\Pi$  state would be of a minor importance.

As a final note, the KED in Fig. 3 extends to a somewhat higher energies than the KED of H fragments from the  $\text{C}_2\text{H}_2$  molecule dissociated directly on the  $\text{Xe}_n$  clusters. This represents quite a different case with respect to the noble gas molecules HXeI and HXeCl observed previously in the gas phase, where the fastest H-fragments from the Xe-containing molecules were always slower than some of the fragments from the direct dissociation of

the HI and HCl molecules on the  $\text{Xe}_n$  cluster. This is in full agreement with the different energetics of the above systems. While the direct dissociation of the HI and HCl molecules can produce fast H-fragments with about 2 eV energy, the dissociation of the corresponding HXeI and HXeCl molecules resulted in a maximum kinetic energy release into the H-fragment of 0.4 eV and 0.7 eV, respectively. In the present case, on the other hand, the dissociation of the HXeCCH can lead to a release of up to 2.3 eV to the H-fragment kinetic energy, while photodissociation of the bare  $\text{C}_2\text{H}_2$  molecule leads to only slow fragments ( $< 0.7$  eV). The vibrational excitation of the  $\text{C}_2\text{H}_2$  molecule by the cage effect in the cluster increases this energy to approximately 1.8 eV, which is still below the 2.3 eV mentioned above.

## VI. CONCLUSIONS

The photolysis of the  $\text{C}_2\text{H}_2$  molecule on  $\text{Xe}_n$  ( $\bar{n} \approx 390$ ) and  $\text{Ar}_n$  ( $\bar{n} \approx 280$ ) clusters has been studied. The photolysis on Xe-clusters resulted in an asymmetric TOF spectrum of the H-fragments, which has been interpreted in terms of *generation*, *orientation*, and subsequent *photodissociation* of a free HXeCCH molecule.

The orientation of the molecule via the pseudo-first-order Stark effect in a strong electric field of the polarized laser light combined with the weak electrostatic field in the extraction region of the time-of-flight spectrometer has been discussed. The molecular parameters, which have been calculated by *ab initio* methods, together with the experimental conditions result in the very high degree of orientation  $\theta_S^0 \approx 26.8$  deg. Other possible species responsible for the spectrum anisotropy, HXeCC, would also exhibit a similar high degree of orientation  $\theta_S^0 \approx 27.0$  deg. However, its generation would require breaking two or more bonds in the  $\text{C}_2\text{H}_2$  molecule with extra photons, which suggests that this species is not the major product of the studied process. Our theoretical calculations suggest the HXeCCH molecule to be quite stable, its dissociation precluded by a barrier of 1.95 eV. On the other hand the analogous Ar-compound, HArCCH, is not stable, which is in agreement with the symmetric shape of the spectra measured for the  $\text{C}_2\text{H}_2/\text{Ar}_n$  system.

Furthermore, the theoretical analysis of the H-fragment kinetic energy distribution after the photolysis of the HXeCCH molecule reveals its dynamics. The molecule is excited by the 193 nm radiation predominantly into the  $2^1\Sigma^+$  state. This state cannot dissociate the Xe-H bond directly, but the system can evolve along the Xe-C coordinate to a conical intersection

of slightly non-linear configuration with the dissociative  $1^1\Pi$  state. This dissociation pathway releases 1.32 eV into the H-fragment kinetic energy, which corresponds approximately to the observed maximum of the measured KED. Part of the molecules can undergo an internal conversion directly after the photoexcitation into the  $1^1\Pi$  state. This process would result in a release of 2.55 eV into the kinetic energy of the H-fragments, which is close to the end of the observed KED spectrum at 2.3 eV.

The oriented HXeCCH molecule has been observed in the gas phase and its photoexcitation studied for the first time.

**Acknowledgment:** Support by the Grant Agency of the Czech Republic Grant Nr.: 203/06/1290, and by the special program "Nanotechnology for society" of the Czech Academy of Sciences grant Nr.: KAN400400461 is gratefully acknowledged. M.F. acknowledges the J.E. Purkyně fellowship of the Czech Academy of Sciences and a support from the Alexander von Humboldt Foundation. P.S. acknowledges support from the postdoctoral grant No. 203/07/P449 and a computational support of Centre for complex molecular systems and biomolecules (LC512).

---

\* Corresponding author. E-mail: `michal.farnik@jh-inst.cas.cz`

† *Also at:* J. Heyrovský Institute of Physical Chemistry, Academy of Sciences of the Czech Republic, Prague 8, Czech Republic; E-mail: `petr.slavicek@vscht.cz`

## References

- <sup>1</sup> N. Bartlett, Proc. Chem. Soc. p. 218 (1962).
- <sup>2</sup> M. Pettersson, J. Lundell, and M. Räsänen, J. Chem. Phys. **102**, 6423 (1995).
- <sup>3</sup> M. Pettersson, J. Lundell, and M. Räsänen, J. Chem. Phys. **103**, 205 (1995).
- <sup>4</sup> L. Khriachtchev, M. Pettersson, N. Runeberg, J. Lundell, and M. Räsänen, Nature **406**, 874 (2000).
- <sup>5</sup> R. B. Gerber, Annu. Rev. Phys. Chem. **55**, 55 (2004).
- <sup>6</sup> M. Pettersson, L. Khriachtchev, J. Lundell, and M. Räsänen, in *Inorganic Chemistry in Focus II*, edited by G. Meyer, D. Naumann, and L. Wesemann (Wiley-VCH, Weinheim, 2005), p. 15.
- <sup>7</sup> W. Grochala, Chemical Society Reviews **36**, 1632 (2007).
- <sup>8</sup> J. Lundell, A. Cohen, and B. Gerber, J. Phys. Chem. A **106**, 11950 (2002).
- <sup>9</sup> L. Khriachtchev, H. Tanskanen, J. Lundell, M. Pettersson, H. Kiljunen, and M. Räsänen, J. Am. Chem. Soc. **125**, 4696 (2003).
- <sup>10</sup> V. I. Feldman, F. F. Sukhov, A. Y. Orlov, and I. V. Tyulpina, J. Am. Chem. Soc. **125**, 4698 (2003).
- <sup>11</sup> L. Khriachtchev, M. Pettersson, J. Lundell, and M. Räsänen, J. Chem. Phys. **114**, 7727 (2001).
- <sup>12</sup> L. Khriachtchev, H. Tanskanen, A. Cohen, R. B. Gerber, J. Lundell, M. Pettersson, H. Kiljunen, and M. Räsänen, J. Am. Chem. Soc. **125**, 6876 (2003).
- <sup>13</sup> A. Cohen, M. Y. Niv, and R. B. Gerber, Faraday Discuss. **118**, 269 (2001).
- <sup>14</sup> R. Baumfalk, N. H. Nahler, and U. Buck, J. Phys. Chem. **114**, 4755 (2001).
- <sup>15</sup> N. H. Nahler, U. Buck, Z. Bihary, R. B. Gerber, and B. Friedrich, J. Chem. Phys. **119**, 224 (2003).
- <sup>16</sup> N. H. Nahler, M. Fárnik, and U. Buck, Chem. Phys. **301**, 173 (2004).
- <sup>17</sup> B. Friedrich, N. H. Nahler, and U. Buck, J. Mod. Opt. **50**, 2677 (2003).
- <sup>18</sup> U. Buck and M. Fárnik, Int. Rev. Phys. Chem. **25**, 583 (2006).
- <sup>19</sup> H. Tanskanen, L. Khriachtchev, J. Lundell, and M. Rasanen, J. Chem. Phys. **125**, 074501

- (2006).
- <sup>20</sup> H. Tanskanen, S. Johansson, A. Lignell, L. Khriachtchev, and M. Rasanen, *J. Chem. Phys.* **127**, 154313 (2007).
- <sup>21</sup> L. Sheng and R. Gerber, *J. Chem. Phys.* **126**, 021108 (2007).
- <sup>22</sup> G. M. Chaban, J. Lundell, and R. B. Gerber, *Chem. Phys. Lett.* **364**, 628 (2002).
- <sup>23</sup> A. Lignell, L. Khriachtchev, J. Lundell, H. Tanskanen, and M. Rasanen, *J. Chem. Phys.* **125** (2006).
- <sup>24</sup> T. Li, Y. Liu, R. Lin, T. Yeh, and W. Hu, *Chem. Phys. Lett.* **434**, 38 (2007).
- <sup>25</sup> T. Ansbacher and R. Gerber, *Phys. Chem. Chem. Phys.* **8**, 4175 (2006).
- <sup>26</sup> U. Buck, *J. Phys. Chem. A* **106**, 10049 (2002).
- <sup>27</sup> O. F. Hagen, *Surf. Sci.* **106**, 101 (1981).
- <sup>28</sup> U. Buck and R. Krohne, *J. Chem. Phys.* **105**, 5408 (1996).
- <sup>29</sup> R. Baumfalk, U. Buck, C. Frischkorn, N. H. Nahler, and L. Hüwel, *J. Chem. Phys.* **111**, 2595 (1999).
- <sup>30</sup> R. Baumfalk, N. H. Nahler, U. Buck, M. Y. Niv, and R. B. Gerber, *J. Chem. Phys.* **113**, 329 (2000).
- <sup>31</sup> B. Friedrich and D. Herschbach, *J. Phys. Chem. A* **103**, 10280 (1999).
- <sup>32</sup> B. Friedrich and D. Herschbach, *J. Chem. Phys.* **111**, 6157 (1999).
- <sup>33</sup> T. Dunning, *J. Chem. Phys.* **90**, 1007 (1989).
- <sup>34</sup> K. Peterson, D. Figgen, E. Goll, H. Stoll, and M. Dolg, *J. Chem. Phys.* **119**, 11113 (2003).
- <sup>35</sup> D. R. Lide (Editor), *CRC handbook of chemistry and physics, internet version 2007, (87th edition)*, <http://www.hbcpnetbase.com>, Taylor and Francis, Boca Raton, FL, 2007.
- <sup>36</sup> S. Minemoto, H. Tanji, and H. Sakai, *J. Chem. Phys.* **119**, 7737 (2003).
- <sup>37</sup> J. Baker, A. Scheiner, and J. Andzelm, *Chem. Phys. Lett.* **216**, 380 (1993).
- <sup>38</sup> R. Dressler and M. Allan, *J. Chem. Phys.* **87**, 4510 (1987).
- <sup>39</sup> M. Prakash, J. Weibel, and R. Marcus, *J. Geophys. Res.* **110**, D21315 (2005).
- <sup>40</sup> M. J. Frisch, G. W. Trucks, H. B. Schlegel, G. E. Scuseria, M. A. Robb, J. R. Cheeseman, J. A. Montgomery, Jr., T. Vreven, K. N. Kudin, J. C. Burant, et al., *Gaussian 03, Revision C.02*, Gaussian, Inc., Wallingford, CT, 2004.
- <sup>41</sup> H.-J. Werner, P. J. Knowles, R. Lindh, F. R. Manby, M. Schütz, P. Celani, T. Korona, G. Rauhut, R. D. Amos, A. Bernhardsson, et al., *Molpro, version 2006.1, a package of ab*

*initio programs* (2006), see <http://www.molpro.net>.

- <sup>42</sup> B. A. Balko, J. Zhang, and Y. T. Lee, *J. Chem. Phys.* **94**, 7958 (1991).
- <sup>43</sup> V. Poterya, M. Fárník, M. Ončák, P. Slavíček, and U. Buck, prepared for publication (2008).
- <sup>44</sup> R. Baumfalk, N. H. Nahler, and U. Buck, *Phys. Chem. Chem. Phys.* **3**, 2372 (2001).
- <sup>45</sup> L. Sheng, A. Cohen, and R. Gerber, *J. Am. Chem. Soc.* **128**, 7156 (2006).
- <sup>46</sup> J. Farges, M. F. de Feraudy, B. Raoult, and G. Torchet, *Sur. Sci.* **106**, 95 (1981).
- <sup>47</sup> P. Slavíček, P. Jungwirth, M. Lewerenz, N. H. Nahler, M. Fárník, and U. Buck, *J. Phys. Chem. A* **107**, 7743 (2003).
- <sup>48</sup> Since two different lasers are used for the C<sub>2</sub>H<sub>2</sub> dissociation and for the H-fragment ionization, different laser fields can interact with the HXeCCH molecule. Their electric fields are parallel, but their intensities differ slightly (see Tab. I). The parameter  $\Delta\omega$  in Tab. II corresponds to the lower laser intensity, since we want to establish the feasibility of the HXeCCH molecule orientation, and to achieve the orientation with the higher field would be even easier.
- <sup>49</sup> Q. Cui, K. Morokuma, and J. Stanton, *Chem. Phys. Lett.* **263**, 46 (1996).
- <sup>50</sup> Q. Cui and K. Morokuma, *Chem. Phys. Lett.* **272**, 319 (1997).

TABLE I: Experimental conditions.

Gas	Ar	Xe
expansion pressure $p_0$ (bar)	6.0	2.9
nozzle temperature $T_0$ (K)	218	248
mean cluster size $\bar{n}$	280	390
Laser intensity	$I_l$ ( $10^{10}\text{Wcm}^{-2}$ )	
$\lambda = 193$ nm	3.3	
$\lambda = 243$ nm	3.1	
Extraction field $\epsilon_S$ ( $\text{Vcm}^{-1}$ )	5.8	

TABLE II: Parameters for the the orientation of molecules:  $\Delta\alpha$  polarizability anisotropy,  $B$  rotational constant,  $\mu$  dipole moment,  $\Delta\omega$  and  $\omega$  are dimensionless parameters defined in Eq. 2 and Eq. 4,  $\langle\cos\theta_s\rangle$  is the directional cosine, and  $\theta_S^0$  is the orientation angle. The molecular parameters  $\Delta\alpha$ ,  $B$ , and  $\mu$  are calculated at MP2 level with aug-cc-pVTZ basis, the open shell molecule HXeCC has been calculated at DFT/B3LYP level with the same basis.

Molecule	$\Delta\alpha/(\text{\AA}^3)$	$B(\text{cm}^{-1})$	$\mu$ (D)	$\Delta\omega$	$\omega$	$\langle\cos\theta_s\rangle$	$\theta_S^0$
$\text{C}_2\text{H}_2$	1.74	1.17	0	0.46	0	0	90
HXeCCH	11.81	0.081	3.41	45.0	0.0041	0.89	26.8
HXeCC	12.13	0.089	5.24	42.5	0.0058	0.89	27.0
HArCCH	15.31	0.118	5.25	40.2	0.0043	0.84	32.7



TABLE III: Energetics (in eV) of decomposition of the HXeCCH molecule at various levels of theory. TS is the transition state.

Method	HXeCCH	TS	HCCH $\cdots$ Xe	H + Xe + CCH
DFT/B3LYP	0.00	2.11	-4.72	1.30
MP2	0.00	2.06	-4.83	1.08
MS-CASPT2 (6/6)	0.00	2.34	-4.63	1.24
MS-CASPT2 (10/10)	0.00	2.30	-4.76	0.81
MRCI (6/6)	0.00	1.95	-4.84	0.92

TABLE IV: Electronic transitions of the HXeCCH and HCCH $\cdots$ Xe systems at various levels of theory in eV. Oscillatory strengths  $f$  at MRCI level are also shown. The ground state is  $1^1\Sigma^+$  for both species, FS denotes the final state.

Species	FS	EOM-CCSD	MS-CASPT2 (6/6)	MS-CASPT2 (10/10)	MRCI (6/6)	$f(\text{MRCI})$
HXeCCH	$1^1\Pi$	5.67	5.80	5.41	5.21	0.0026
	$2^1\Pi$	6.75	6.99	6.72	6.53	0.030
	$2^1\Sigma^+$	6.30	6.34	6.15	6.37	0.23
	$3^1\Sigma^+$	6.73	6.97	6.75	6.77	0.85
HCCH $\cdots$ Xe	$1^1\Sigma^-$	7.03	6.87	6.83	7.00	0.00
	$2^1\Sigma^-$	7.34	7.22	7.19	7.34	0.00
	$2^1\Sigma^+$	7.34	7.26	7.24	7.31	0.00

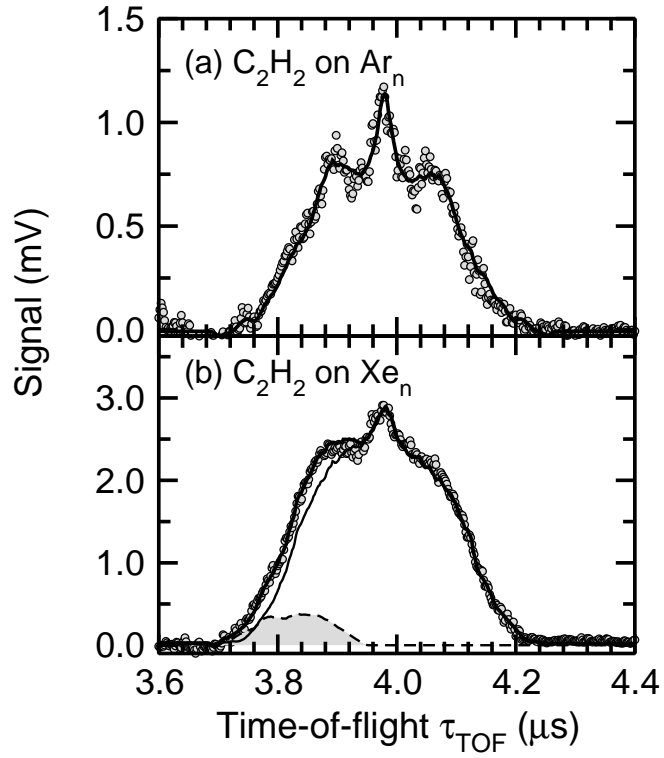


FIG. 1: TOF spectra of H-fragments from photolysis of acetylene on  $\text{Ar}_n$   $\bar{n} = 280$  (a), and  $\text{Xe}_n$ ,  $\bar{n} = 390$ , clusters (b). The bottom spectrum was simulated with a symmetric part (thin line) and an asymmetric part (dashed line, shaded area), which indicates photolysis of an oriented  $\text{HXeCCH}$  molecule.

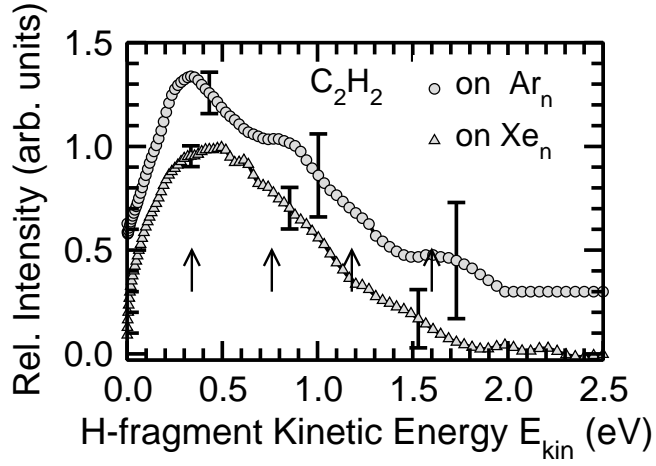


FIG. 2: KEDs of the H-fragments from the photolysis of acetylene on  $\text{Ar}_n$ ,  $\bar{n} = 280$ , (circles) and  $\text{Xe}_n$ ,  $\bar{n} = 390$ , (triangles) clusters. The latter KED has been obtained by the fit of the symmetric part of the TOF spectrum in Fig. 1 (b). Both spectra have been normalized to the same area and the upper one has been arbitrarily shifted in the y-axis direction for a better clarity.

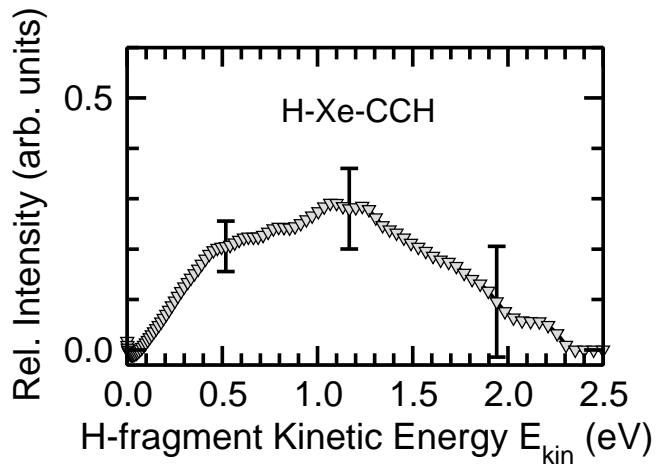


FIG. 3: KED of the H-fragments from the photolysis of the  $\text{HXeCCH}$  molecule generated by the photodissociation of acetylene on  $\text{Xe}_n$ ,  $\bar{n} = 390$ . The KED corresponds to the fit of the asymmetric part of the TOF in Fig. 1 (b).

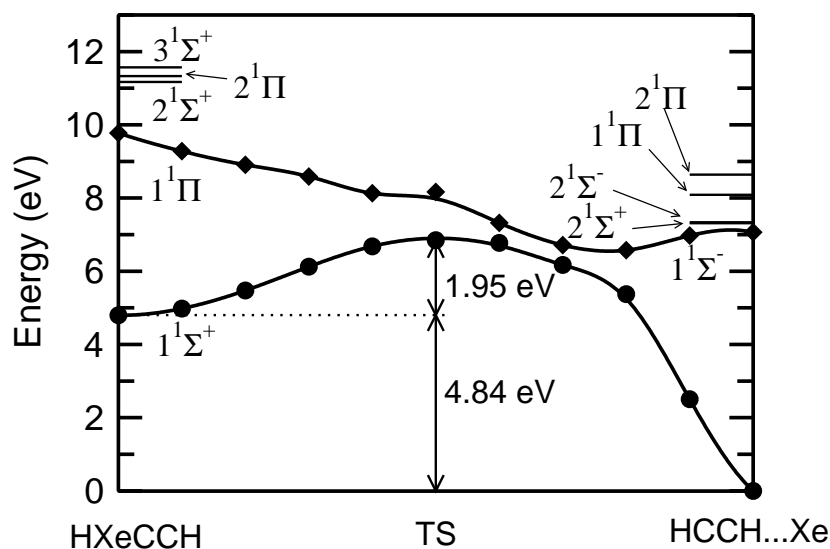


FIG. 4: Linear interpolation in internal coordinates between the HXeCCH molecule, the transition state and the HCCH $\cdots$ Xe complex for ground and first adiabatic states. Indicated is also position of higher excited states. Energies are calculated at MRCI level with 6/7 active space using  $C_s$  symmetry with Davidson correction. The bond lengths in the HXeCCH molecule optimized at the MS-CASPT2 level are close to the previously reported CCSD(T) results,<sup>8</sup> namely 1.82, 2.38, 1.25 and 1.08 Å for H-Xe, Xe-C, C-C and C-H bonds, respectively. For Xe $\cdots$ HCCH molecule, the Xe-H distance is 3.15 Å. Geometrical parameters for the transition state are following: bond lengths are 1.60, 2.95, 1.27 and 1.05 Å for H-Xe, Xe-C, C-C and C-H bonds, H-Xe-C angle is 98.6°.

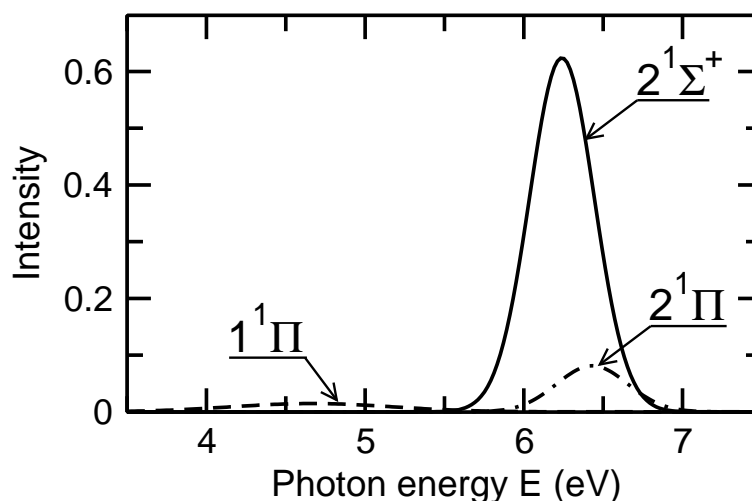


FIG. 5: Absorption spectra of the HXeCCH species calculated at MRCI level with 6/6 active space for the three excited states:  $1^1\Pi$  (dashed line),  $2^1\Sigma^+$  (full line) and  $2^1\Pi$  (dashed-dotted line).

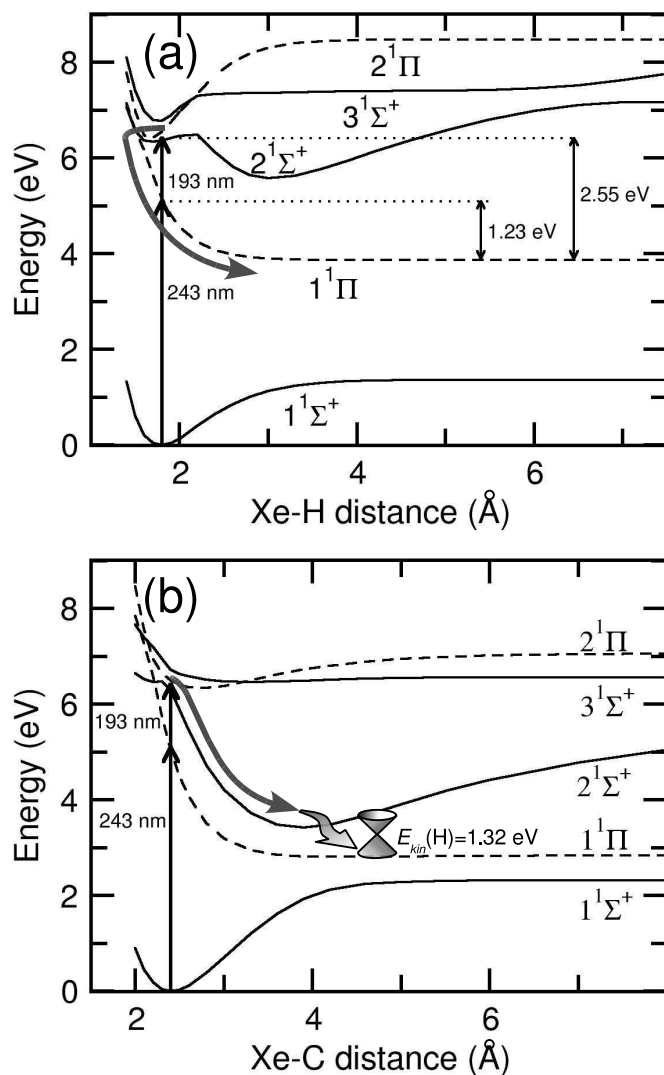


FIG. 6: Potential energy scans along the H-Xe and Xe-C coordinates for the HXeCCH molecule. After the photoexcitation with the 193 nm laser pulse,  $2^1\Sigma^+$  state is dominantly populated. Part of the wavepacket transfers directly into the dissociative  $1^1\Pi$  state, most of the wavepacket deposits the energy into the acetylene moiety before the hydrogen dissociates. All energies are calculated at MRCI level with 6/6 active space in  $C_{2v}$  symmetry with Davidson correction .